

Supplementary Information

Engineering of a bis-chelator motif into a protein α -helix for rigid lanthanide binding and paramagnetic NMR spectroscopy

James D. Swarbrick, Phuc Ung, Xun-Cheng Su, Ansis Maleckis, Sandeep Chhabra, Thomas Huber, Gottfried Otting, and Bim Graham

<i>Contents</i>	<i>Page</i>
Synthesis and characterisation of tagging agent 1	S3
Expression and purification of human ubiquitin mutants	S4
Tagging of proteins	S4
Protein NMR spectroscopy	S5
Metal position and tensor determination from PCSs	S6
Figure S1. ^{15}N -HSQC spectra of ArgN-NTA with Dy^{3+} , Tm^{3+} , and Yb^{3+}	S7
Figure S2. ^{15}N -HSQC spectrum of ArgN-NTA with Co^{2+}	S9
Figure S3. ^{15}N -HSQC spectra of UbiquA28C-NTA with Dy^{3+} , Tb^{3+} , Tm^{3+} , and Yb^{3+}	S10
Figure S4. ^{15}N -HSQC spectra of UbiquE24C/A28C-NTA ₂ with Dy^{3+} , Tb^{3+} , Tm^{3+} , and Yb^{3+}	S11
Table S1. Axial and rhombic components of the $\Delta\chi$ tensor of different lanthanides ions in complex with ArgN-NTA	S12
Figure S5. Model of the ArgN-NTA- Ln^{3+} complex	S12
Table S2. Axial and rhombic components of the $\Delta\chi$ tensor of different lanthanides ions in complex with UbiquA28C-NTA	S13
Table S3. Axial and rhombic components of the $\Delta\chi$ tensor of different lanthanides ions in complex with UbiquE24C/A28C-NTA ₂	S14
Figure S6. Model of the UbiquE24C-A28C-NTA ₂ - Ln^{3+} complex	S14
Figure S7. Correlation between measured and back-calculated PCSs for ArgN-NTA- Ln^{3+} complexes	S15



Figure S8. Correlation between measured and back-calculated PCSs for UbiqE24C-NTA-Ln ³⁺ complexes	S16
Figure S9. Correlation between measured and back-calculated PCSs for UbiqE24C/A28C-NTA ₂ -Ln ³⁺ complexes	S17
Figure S10. Comparison of measured ¹ D _{HN} RDCs and those calculated from the Δχ tensor for the UbiqE24C/A28C-NTA ₂ -Tm ³⁺ complex	S18
Figure S11. Comparison of measured ¹ D _{HN} RDCs and those calculated for the UbiqE24C/A28C-NTA ₂ -Tm ³⁺ complex recorded at a field strength of 14.1 Tesla	S19
Figure S12. Comparison of the principal axes of the Δχ tensor with those of the RDC-derived alignment tensor for the UbiqE24C/A28C-NTA ₂ -Tm ³⁺ complex, and calculation of the axial component of the RDC-derived Δχ tensor	S20
Table S4. Experimentally measured H ^N PCSs (in ppm) for ArgN-NTA-Ln ³⁺ complexes	S21
Table S5. Experimentally measured H ^N PCSs (in ppm) for UbiqA28C-NTA-Ln ³⁺ complexes	S22
Table S6. Experimentally measured H ^N PCSs (in ppm) for UbiqE24C/A28C-NTA ₂ -Ln ³⁺ complexes	S24
Table S7. Experimentally measured ¹ D _{HN} RDCs (in Hz) for UbiqE24C/A28C-NTA ₂ -Tm ³⁺ complex	S26
References	S27

Synthesis and characterisation of tagging agent 1

All starting materials, reagents and solvents were obtained from commercial suppliers and were of general reagent grade or analytical grade and used without further purification unless stated otherwise.

***N*^α-(*t*-butoxycarbonylmethyl)-*S*-trityl-*L*-cysteine-*O*-*tert*-butyl ester and *N*^α,*N*^α-bis(*t*-butoxycarbonylmethyl)-*S*-trityl-*L*-cysteine-*O*-*tert*-butyl ester.** To a solution of *S*-trityl-*L*-cysteine-*O*-*tert*-butyl ester¹ (2.20 g, 5.24 mmol) in dry *N,N*-dimethylformamide (20 mL) was added *tert*-butyl bromoacetate (3.90 g, 20.0 mmol) and diisopropylethylamine (2.58 g, 20.0 mmol). The reaction mixture was stirred at room temperature for 12 h and another 6 h at 50 °C. Volatiles were then removed under reduced pressure and the residue dissolved in ethyl acetate (200 mL). The solution was extracted with saturated aq. NH₄Cl solution (2 x 100 mL) and brine (2 x 150 mL), and the organic phase dried over anhydrous sodium sulfate, filtered and concentrated under reduced pressure. Column chromatography of the residue (silica gel; mobile phase: ethyl acetate/hexane with gradient from 1:20 to 1:4 v/v) yielded *N*^α,*N*^α-bis(*t*-butoxycarbonylmethyl)-*S*-trityl-*L*-cysteine-*O*-*tert*-butyl ester (1.75 g; 52%) as a thick colourless oil.

¹H-NMR δ_H (300 MHz, CDCl₃): 7.35 (6H, d, *J* = 7.6 Hz), 7.17 (9H, m), 3.32 (2H, d, *J* = 18.5 Hz), 3.26 (2H, d, *J* = 18.5 Hz), 2.87 (1H, dd, *J* = 8.8, 6.5 Hz), 2.51 (1H, dd, *J* = 12.9, 8.8 Hz), 2.33 (1H, dd, *J* = 12.9, 6.5 Hz), 1.34 (9H, s), and 1.33 (18H, s).

***N*^α,*N*^α-bis(carboxymethyl)-*L*-cysteine hydrochloride.** *N*^α,*N*^α-bis(*t*-butoxycarbonylmethyl)-*S*-trityl-*L*-cysteine-*O*-*tert*-butyl ester (1.30 g, 2.01 mmol) was dissolved in dry dichloromethane (10 mL) under a nitrogen atmosphere, and then triethylsilane (930 mg, 8.00 mmol) and 1,2-ethanedithiol (754 mg, 8.00 mmol) were added. After cooling to -5 °C, trifluoroacetic acid (15 mL) was added in a dropwise fashion. The reaction mixture was then stirred at room temperature for 12 h, after which time the volatiles were removed under reduced pressure. Hydrogen chloride solution in diethyl ether (2 M; 10 mL) was added and the resulting suspension stirred at room temperature for 5 min. Volatiles were again removed under reduced pressure and this procedure repeated a further three times. The crystalline residue was then suspended in diethyl ether (15 mL) under a nitrogen atmosphere, and the suspension stirred for 5 min. The liquid phase was decanted and this procedure repeated four times. The remaining residue was dried under reduced pressure to yield the final product (320 mg, 58%) as a hygroscopic white powder. According to ¹H-NMR the product contains 20–30% of the corresponding disulfide. It was used without further purification.

¹H-NMR δ_H (300 MHz, D₂O): 3.84 (5H, m), 3.02 (1H, dd, *J* = 14.5, 6.4 Hz) and 2.86 (1H, dd, *J* = 14.5, 7.7 Hz).

¹³C-NMR δ_C (100 MHz, D₂O): 171.63, 171.24, 67.91, 54.15, and 21.68.

HRMS (TOF-ES⁺) [M-H]⁺: calculated C₇H₁₀NO₆S 236.0229, found 236.0228.

Expression and purification of human ubiquitin mutants

pET28a plasmids containing the synthesized gene sequences (Geneart) of the human ubiquitin mutant A28C or E24C/A28C were cloned with an N-terminal His₆ tag and a thrombin cleavage site. *E. coli* BL21 (DE3) cells transformed with the plasmid were grown overnight in 3 mL of 2×YT media supplemented with 100 µg mL⁻¹ kanamycin for selection. The overnight culture was subcultured into 50 mL of minimal media that was grown to an OD₆₀₀ of 0.5–0.7. This was then added to 1 L of minimal media supplemented with 1.5 g ¹⁵N ammonium chloride and grown at 310 K until the OD₆₀₀ was 0.5–0.8. Isopropyl β-D-1-thiogalactopyranoside (IPTG) was added to a final optimised concentration of 0.5 mM and expression was carried out at 293 K for 12 h. The cultures were centrifuged at 5,000 g at 278 K for 10 min and the cells then re-suspended in 100 mL of 50 mM HEPES, 5% glycerol, pH 8.0. An EDTA-free Complete™ protease inhibitor cocktail tablet (Roche) was added along with lysozyme, the latter to a final concentration of 0.2 mg mL⁻¹. Cells were sonicated and cell debris removed by centrifugation at 18,000 g for 30 min. The supernatant was loaded onto a Ni-NTA IMAC column (Qiagen) and unbound protein washed off with 10 mM imidazole in 50 mM HEPES-NaOH buffer, 0.3 M NaCl, pH 8.0. The His-tagged protein was eluted from the IMAC column with 250 mM imidazole in HEPES-NaCl buffer. Fractions were analysed using a 15% SDS-PAGE gel with Coomassie staining and protein-containing fractions were pooled, buffer exchanged into 20 mM HEPES, pH 7.0, and concentrated to 2.0 mg mL⁻¹ using a 3 kDa molecular-weight cut-off ultrafiltration centrifugal device (Amicon).

Tagging of proteins

For each of the ubiquitin mutants, DTT (10 mM) was added to ¹⁵N-labelled sample and gently mixed for 1 h at room temperature. A PD10 column (GE Healthcare) equilibrated with fresh degassed 50 mM HEPES, pH 7.5, was used to remove the DTT. 5,5'-Dithiobis(2-nitrobenzoic acid) (DTNB, 10 equivalents) stock suspended in water was pipetted into the protein solution slowly with gentle mixing. An immediate color change from clear to intense yellow was observed. The reaction was allowed to proceed at room temperature for 20 minutes. The mixture was subsequently eluted through a PD10 column to remove excess DTNB from the solution. **1** (10 equivalents) was added slowly with gentle mixing. An immediate color change to yellow was observed again. The sample was allowed to stand at room temperature for 5 h. Excess **1** was then removed *via* the use of a PD10 column. ¹⁵N-HSQC NMR spectroscopy was used to monitor the progress of all steps (i.e. DTNB activation and reaction with **1**). As the reactions were observed to proceed to completion *via* NMR, no further chromatographic purification was performed.

For the N-terminal domain of the *E. coli* arginine repressor (ArgN),² a uniformly ¹⁵N-labeled sample of the protein was treated with DTNB to activate Cys68, followed by reaction with **1** as described previously.³ The tagged protein was purified by FPLC on a mono SP ion exchange column.

Protein NMR spectroscopy

Ubiquitin mutants:

0.4 mM solutions of $^{13}\text{C}/^{15}\text{N}$ -labeled ubiquitin mutant(A28C or E24C/A28C) in NMR buffer (25 mM HEPES, pH 7.0) were prepared. NMR experiments were run on a Varian Inova 600 MHz NMR spectrometer equipped with a cryoprobe and a z axis gradient operating at 298 K. The backbone $^1\text{H}^{\text{N}}$, ^{15}N , $^{13}\text{C}^{\alpha}$ and side chain $^{13}\text{C}^{\beta}$ resonances were assigned using the HNCACB and CBCA(CO)NH experiments.⁴ Resonance assignments for the UbiqA28C-NTA- La^{3+} complex was verified using a 3D NOESY- ^{15}N -fastHSQC experiment recorded with a 200ms mixing time on a 200 μM ^{15}N -labeled sample in the presence of 500 μM La^{3+} .

For PCS measurements, NMR spectra were recorded of ~ 100 μM solutions of UbiqA28C-NTA/UbiqE24C/A28C-NTA₂ in the simultaneous presence of 60 μM La^{3+} and 60 μM of one of the following lanthanide ions: Tb^{3+} , Dy^{3+} , Tm^{3+} , or Yb^{3+} . soFast HMQC⁵ and fastHSQC⁶ experiments were acquired with $t_{1\text{max}}(^{15}\text{N}) = 41$ and 72 ms, respectively, and $t_{2\text{max}}(^1\text{H}) = 122$ ms. $^1D_{\text{HN}}$ RDC measurements of the UbiqE24C/A28C-NTA₂- Tb^{3+} complex were performed by measuring the difference in the doublet splittings measured in the ^{15}N dimension in a ^{15}N FastHSQC experiment (recorded without decoupling in the ^{15}N dimension), using a UbiqE24C/A28C-NTA₂- $\text{Tb}^{3+}/\text{La}^{3+}$ sample. Acquisition times were $t_{1\text{max}}(^{15}\text{N}) = 72$ ms and $t_{2\text{max}}(^1\text{H}) = 244$ ms, respectively. All NMR spectra were processed using nmrPipe.⁹ Xeasy¹⁰ was used for backbone assignments and PCS and RDC values were measured using Sparky.¹¹

ArgN:

For measurements of PCSs, 0.13 mM solutions of ^{15}N -labeled ArgN-NTA- Ln^{3+} in NMR buffer (20 mM MES, pH 6.5) in the presence of 0.08 mM Y^{3+} and 0.08 mM paramagnetic lanthanide(Dy^{3+} , Tb^{3+} , Tm^{3+} , or Yb^{3+}) were prepared. NMR experiments were acquired at 298 K on a Bruker Avance 600 MHz NMR spectrometer equipped with a TCI-cryoprobe and a z axis gradient. The resonance assignments of the ArgN-NTA- Y^{3+} complex and the structural integrity of the protein were verified by a 3D NOESY- ^{15}N -HSQC spectrum (60 ms mixing time), using a 0.3 mM sample. Any chemical shift changes were confined to the vicinity of Cys68.

Metal position and tensor determination from PCSs

All $\Delta\chi$ tensors and metal positions were calculated from the PCS values using the first conformer of the NMR structures of human ubiquitin (PDB code 1D3Z)¹² and the N-terminal domain of the *E. coli* arginine repressor (PDB code 2AOY)² according to Eq. 1¹³ using the program Numbat¹⁴ and PyParaTools.¹⁵

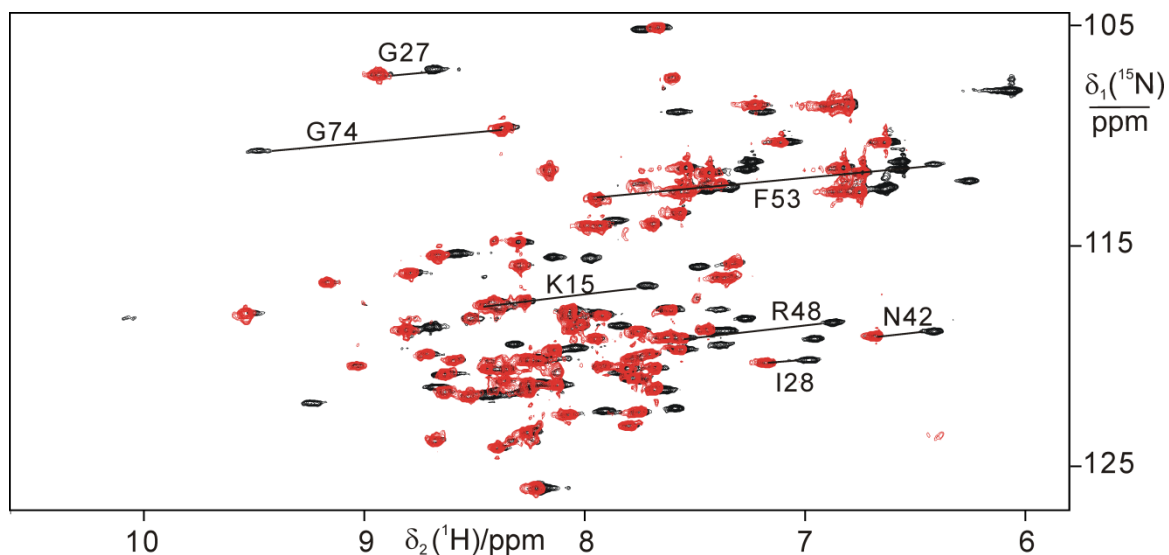
$$\Delta\delta^{\text{PCS}} = \frac{1}{12\pi r^3} \left[\Delta\chi_{\text{ax}} (3\cos^2\theta - 1) + \frac{3}{2} \Delta\chi_{\text{rh}} \sin^2\theta \cos 2\varphi \right] \quad (1)$$

where $\Delta\delta^{\text{PCS}}$ is the pseudocontact shift and the polar coordinates of the nucleus with respect to the principal axes of the magnetic susceptibility tensor are given by r , θ , and ϕ , and $\Delta\chi_{\text{ax}}$ and $\Delta\chi_{\text{rh}}$ are the axial and rhombic components of the anisotropic magnetic susceptibility difference tensor between the diamagnetic and the paramagnetic state.

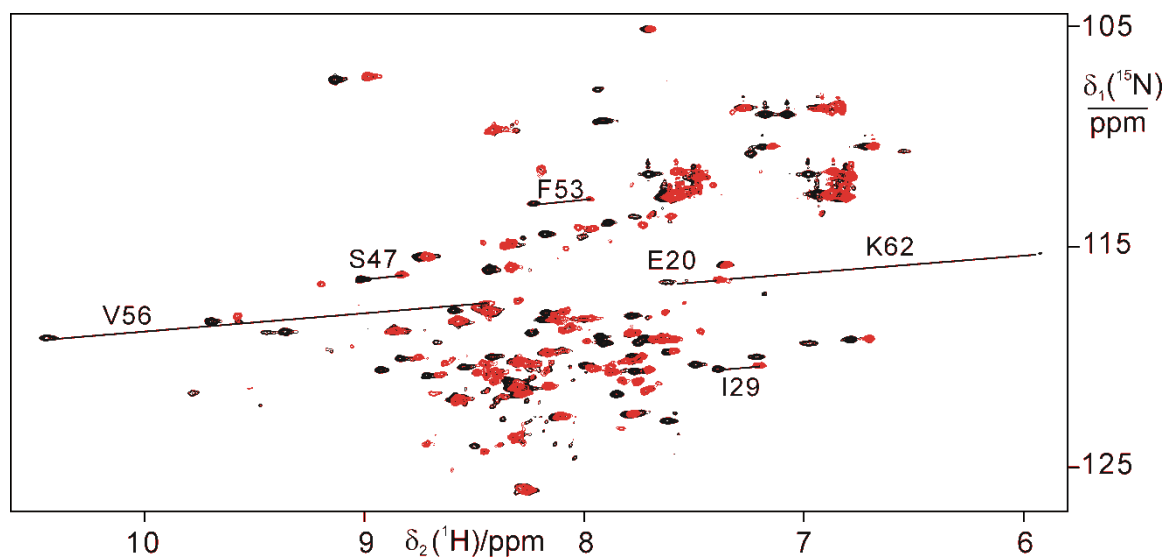
Figure S1. ^{15}N -HSQC spectra of ArgN-NTA with Dy^{3+} , Tm^{3+} , and Yb^{3+}

Superimposition of ^{15}N -HSQC spectra of uniformly ^{15}N -labeled ArgN derivatized with **1** at Cys68 in the presence of a 1:1 mixture of Y^{3+} and paramagnetic lanthanide (black) and in the presence of Y^{3+} (red). The ratio of lanthanides to protein was about 1.2:1. The spectra were recorded at 25 °C and pH 6.5 at a ^1H NMR frequency of 600 MHz. The paramagnetic lanthanide is (a) Dy^{3+} , (b) Tm^{3+} , and (c) Yb^{3+} .

a)



b)



c)

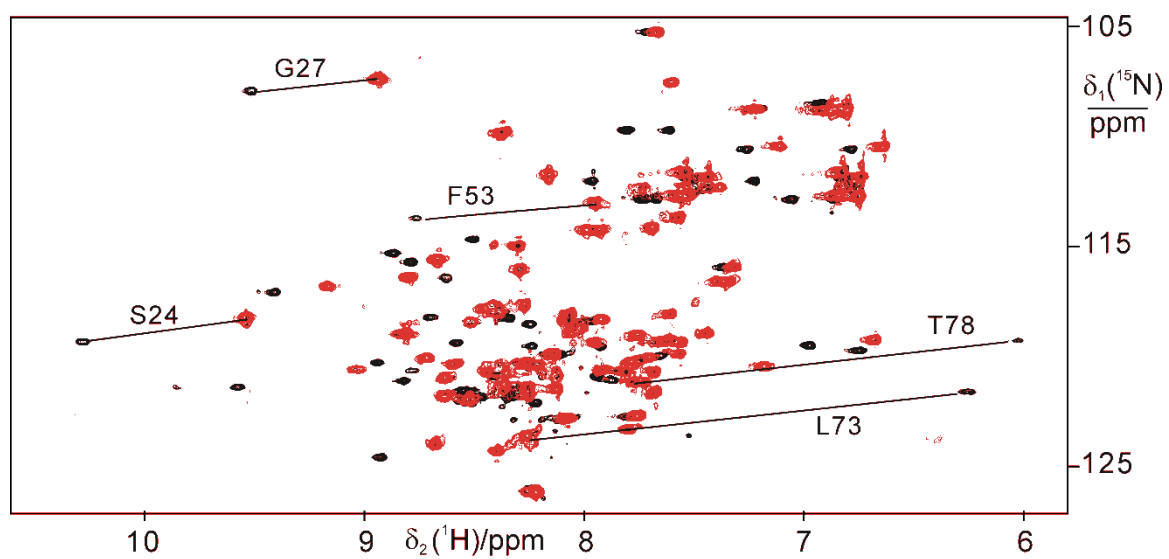


Figure S2. ^{15}N -HSQC spectrum of ArgN-NTA with Co^{2+}

Superimposition of ^{15}N -HSQC spectra of uniformly ^{15}N -labeled ArgN derivatized with **1** at Cys68 in the presence of a 1:1 mixture of Zn^{2+} and Co^{2+} (black) and in the presence of Zn^{2+} (red). All other parameters were as in Figure S1.

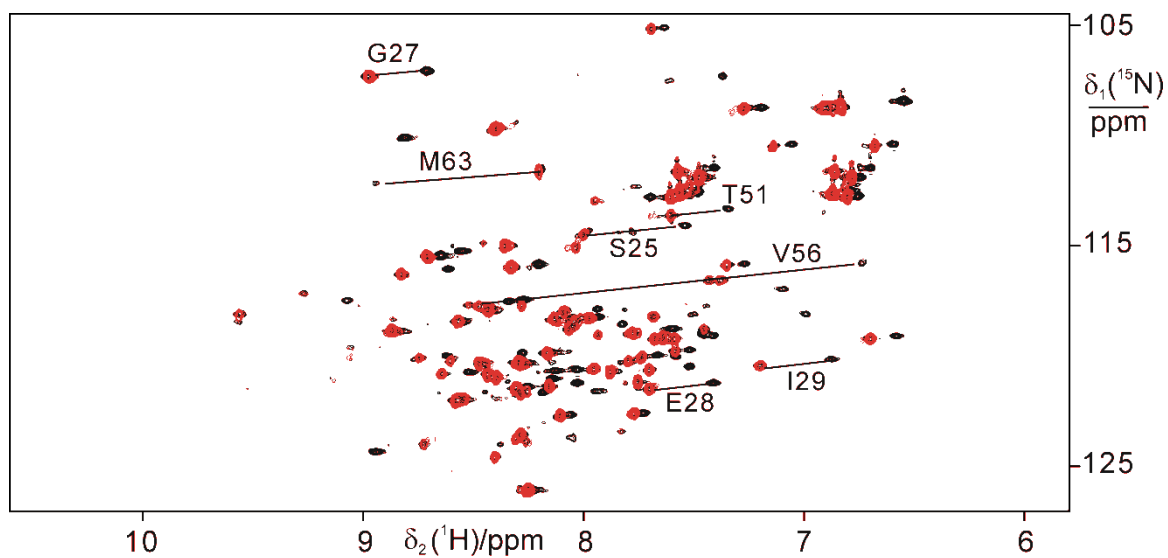


Figure S3. ^{15}N -HSQC spectra of UbiquA28C-NTA with Dy^{3+} , Tb^{3+} , Tm^{3+} , and Yb^{3+}

Superimposition of ^{15}N -HSQC spectra of 100 μM UbiquA28C-NTA in complex with 60 μM La^{3+} and 60 μM Ln^{3+} , where Ln^{3+} is Dy^{3+} (magenta), Tb^{3+} (green), Tm^{3+} (blue), Yb^{3+} (red), or La^{3+} (black).

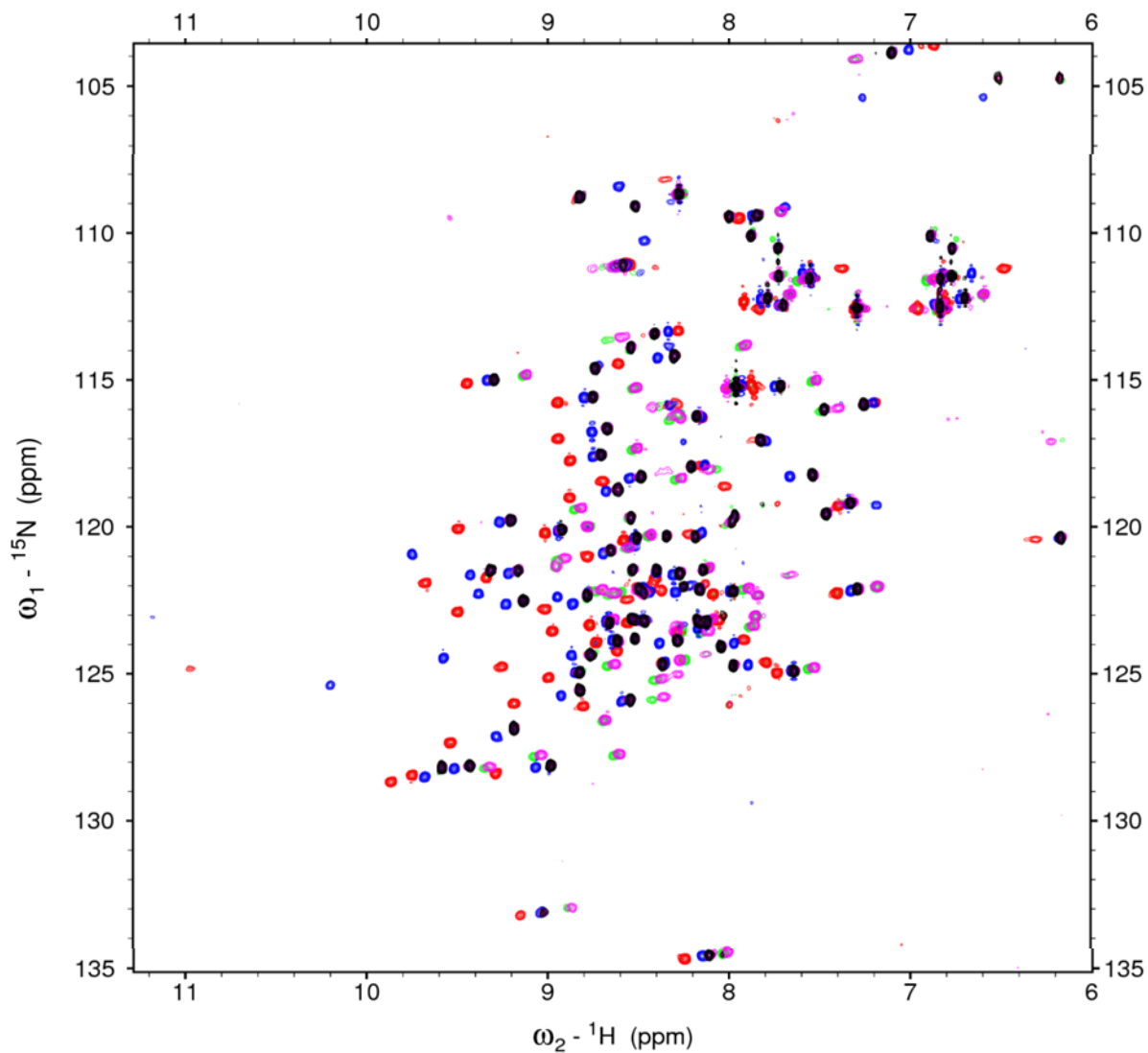


Figure S4. ^{15}N -HSQC spectra of UbiquE24C/A28C-NTA₂ with Dy³⁺, Tb³⁺, Tm³⁺, and Yb³⁺

Superimposition of ^{15}N -HSQC spectra of 100 μM UbiquE24C/A28C-NTA₂ in complex with 60 μM La³⁺ and 60 μM Ln³⁺, where Ln³⁺ is Dy³⁺ (magenta), Tb³⁺ (green), Tm³⁺ (red), Yb³⁺ (blue), or La³⁺ (black).

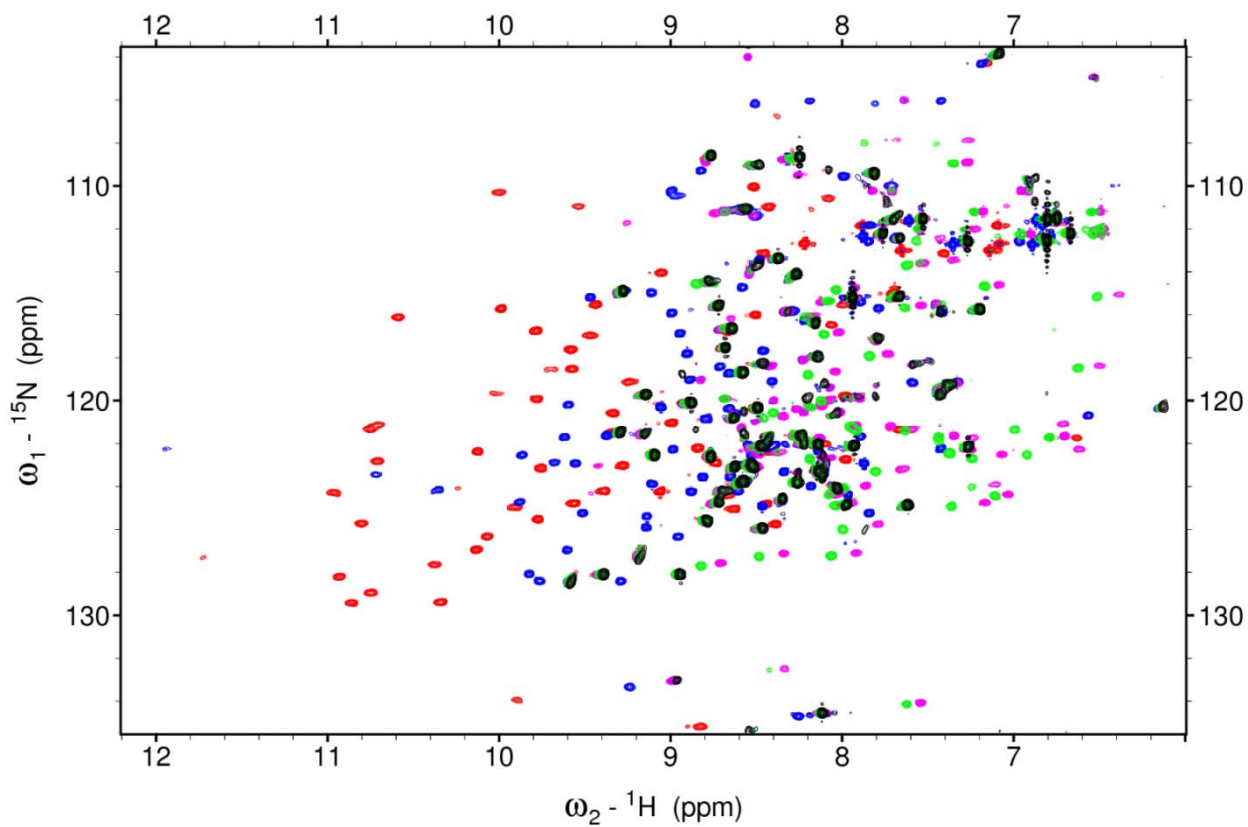


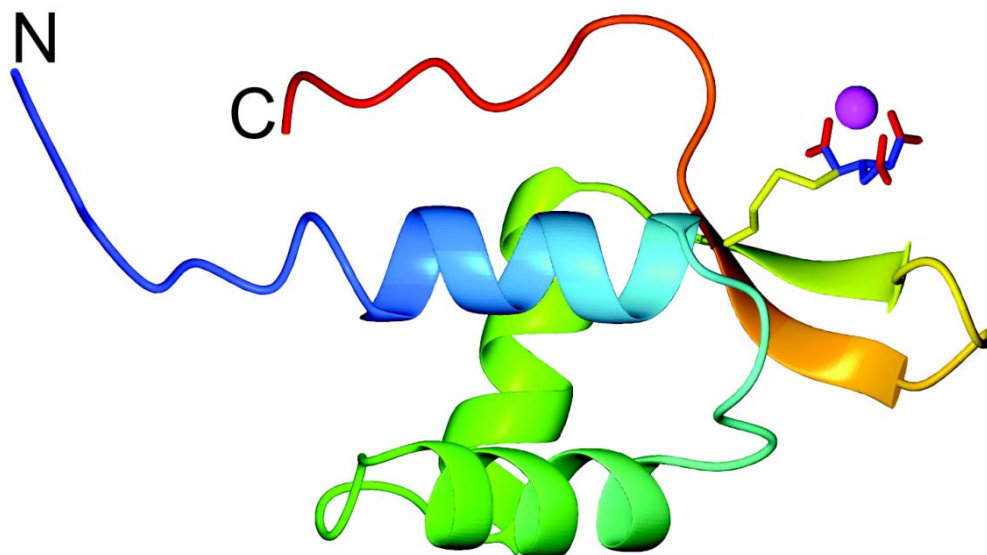
Table S1. Axial and rhombic components of the $\Delta\chi$ tensor of different paramagnetic metal ions bound to ArgN-NTA

	Co ²⁺	Dy ³⁺	Tb ³⁺	Tm ³⁺	Yb ³⁺
$\chi_{ax}/10^{-32}\cdot\text{m}^3$	-5.5	-23.4	-23.7	19.1	5.7
$\chi_{rh}/10^{-32}\cdot\text{m}^3$	-3.2	-7.2	-3.0	10.2	3.7

All five tensors were fitted simultaneously to the first conformer of the NMR structure of the N-terminal domain of the *E. coli* arginine repressor (PDB code 1AOY)² as described below, using a common metal position at $x = 11.482$, $y = 11.635$, $z = 3.077$.

Figure S5. Model of the ArgN-NTA-Ln³⁺ complex

A crystal structure of the Gd-NTA₂ complex (CSD ID BERHIQ)¹⁶ was used to define the geometry of the NTA-Ln complex. The NTA tag was modelled in three different ways by attaching the CH₂-S moiety to each of the three acetate groups of the NTA-Ln structure. The modelled NTA-tags were subsequently crafted onto the side chain of Cys68 via a disulfide bond. Finally, the five dihedral angles of the rotatable bonds connecting the C^α atom of Cys68 with the NTA moiety were randomly varied to generate 10,000 conformers for each of the three NTA models. After removal of all models displaying steric clashes, the $\Delta\chi$ tensors were fitted to each remaining model. The values reported in Table S1 pertain to the model with the lowest overall quality factor that was calculated as the sum of the quality factors Q_i for each metal ion i , where $Q_i = \Sigma(\delta_{\text{exp}}^{\text{PCS}} - \delta_{\text{calc}}^{\text{PCS}})^2 / \Sigma(\delta_{\text{exp}}^{\text{PCS}})^2$ and the sums run over all PCSs observed and back-calculated for the metal ion.¹⁷



The protein is shown as a ribbon, the side chain of Cys68 with the attached NTA tag as sticks, and the lanthanide as a ball.

Table S2. Axial and rhombic components of the $\Delta\chi$ tensor of different lanthanides ions in complex with UbiquA28C-NTA

	Dy ³⁺	Tb ³⁺	Tm ³⁺	Yb ³⁺
$\chi_{ax}/10^{-32}\cdot\text{m}^3$	6.9	6.0	-4.2	-1.1
$\chi_{rh}/10^{-32}\cdot\text{m}^3$	1.2	2.1	-2.2	-0.6

Dy³⁺, Tb³⁺, and Tm³⁺ tensors were fitted simultaneously to the first conformer of the NMR structure of human ubiquitin (PDB code 1D3Z)¹² using a common metal position at x = 4.4, y = 2.3, z = -11.4. Close range PCSs were given large tolerances (+/-0.2 ppm) to allow for motion of the tag that would otherwise skew the tensor fitting.

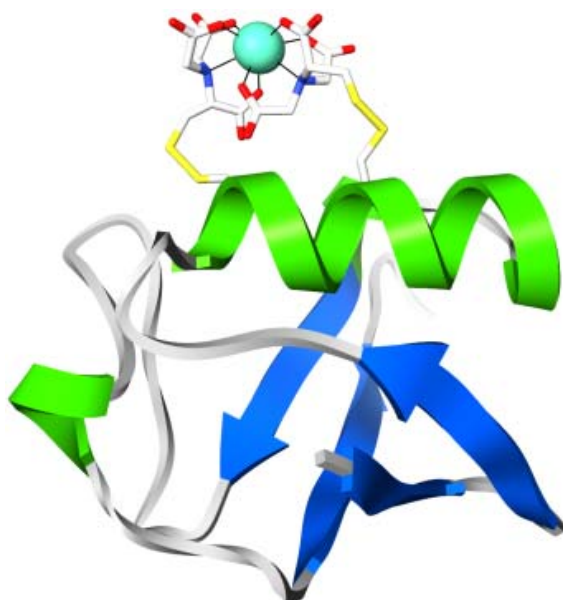
Table S3. Axial and rhombic components of the $\Delta\chi$ tensor of different lanthanide ions in complex with UbiquE24C/A28C-NTA₂

	Dy ³⁺	Tb ³⁺	Tm ³⁺	Yb ³⁺
$\chi_{ax}/10^{-32}\cdot\text{m}^3$	-21.0	-18.1	27.8	6.2
$\chi_{rh}/10^{-32}\cdot\text{m}^3$	-12.9	-10.5	3.0	2.0

All five tensors were fitted simultaneously to the first conformer of the NMR structure of human ubiquitin (PDB code 1D3Z)¹² using a common metal position at $x = 64.287$, $y = -86.448$, $z = -8.821$.

Figure S6. Model of the UbiquE24C/A28C-NTA₂-Ln³⁺ complex

The UbiquE24C/A28C-NTA₂-Ln³⁺ complex was modelled similarly to the model of ArgN-NTA-Ln³⁺ complex. The NTA tag was modelled in three different ways by attaching the CH₂-S moiety to each of the three acetate groups of the NTA-Ln structure. For each of the labelling sites, Cys24 and Cys28, the modelled NTA-tags were subsequently crafted onto the side chain via a disulfide bond, and the five dihedral angles of the rotatable bonds connecting the C^α atom of the cysteine with the NTA moiety were randomly varied to generate 10,000 conformers for each of the three NTA models. After removal of all models displaying steric clashes, the 50 models with the lowest overall quality factor from each labelling site were selected and then pair-wise combined. From the resulting 2,500 models, the model that placed the metal ion positions defined by the two NTA tags closest and which had no steric overlap between atoms in the NTA moieties was selected as the final model. Finally, the $\Delta\chi$ tensors were fitted to the average position of the metal ion position defined by the model rotamer position of the two NTA tags. Alternate tag conformations were found that produced a very similar metal ion position. The final metal ion position was displaced by less than 0.15 Å from the position found by a simultaneous $\Delta\chi$ tensor fit of all four PCS data sets using no constraints imposed by the NTA tags.



The protein is shown as a ribbon, the side chains of Cys24 and Cys28 with the attached NTA tags as sticks, and the lanthanide as a ball.

Figure S7. Correlation between measured and back-calculated PCSs for ArgN-NTA-Ln³⁺(or Co²⁺) complexes

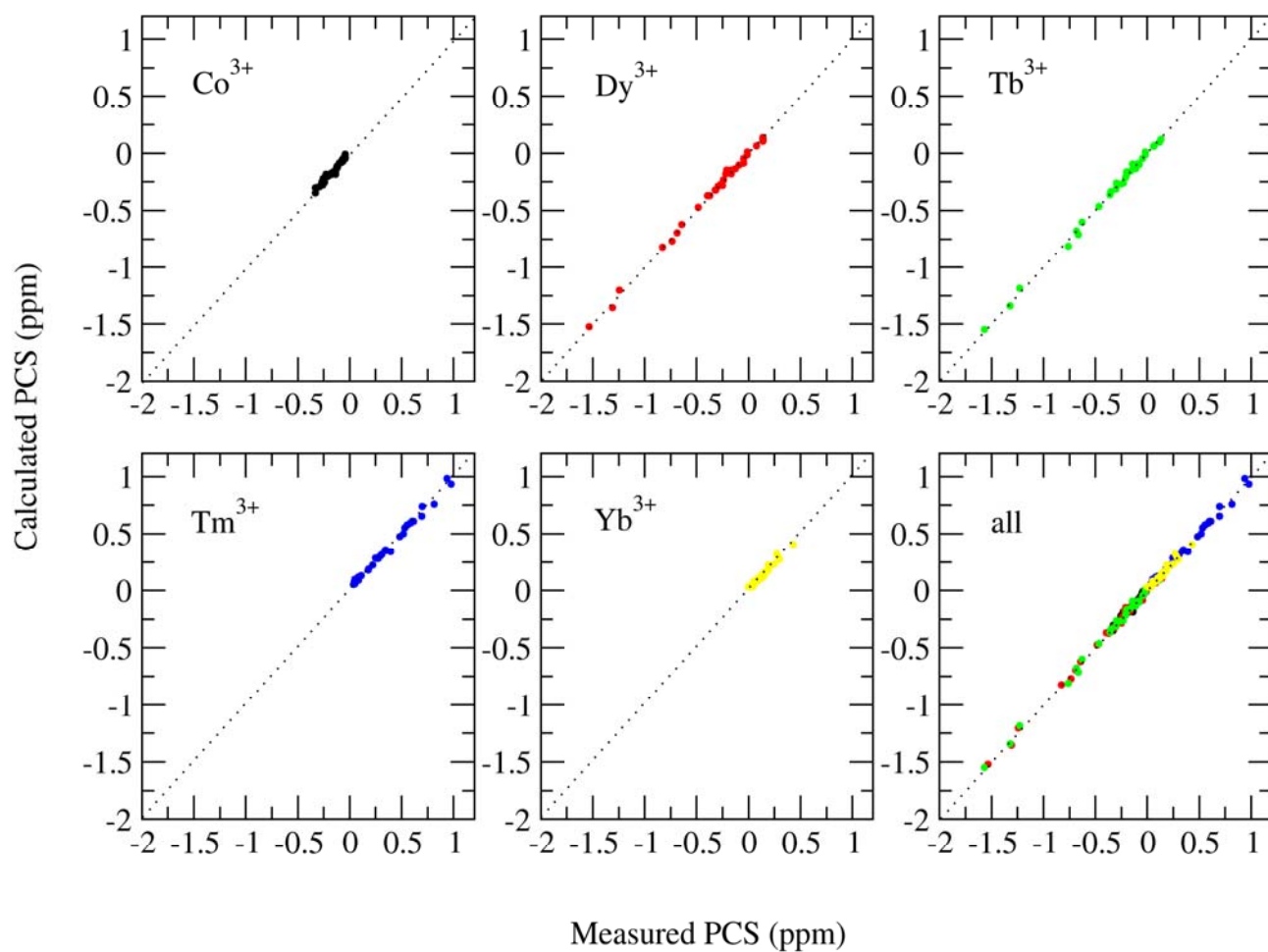


Figure S8. Correlation between measured and back-calculated PCSs for the UbiqE24C/NTA-Ln³⁺ complexes

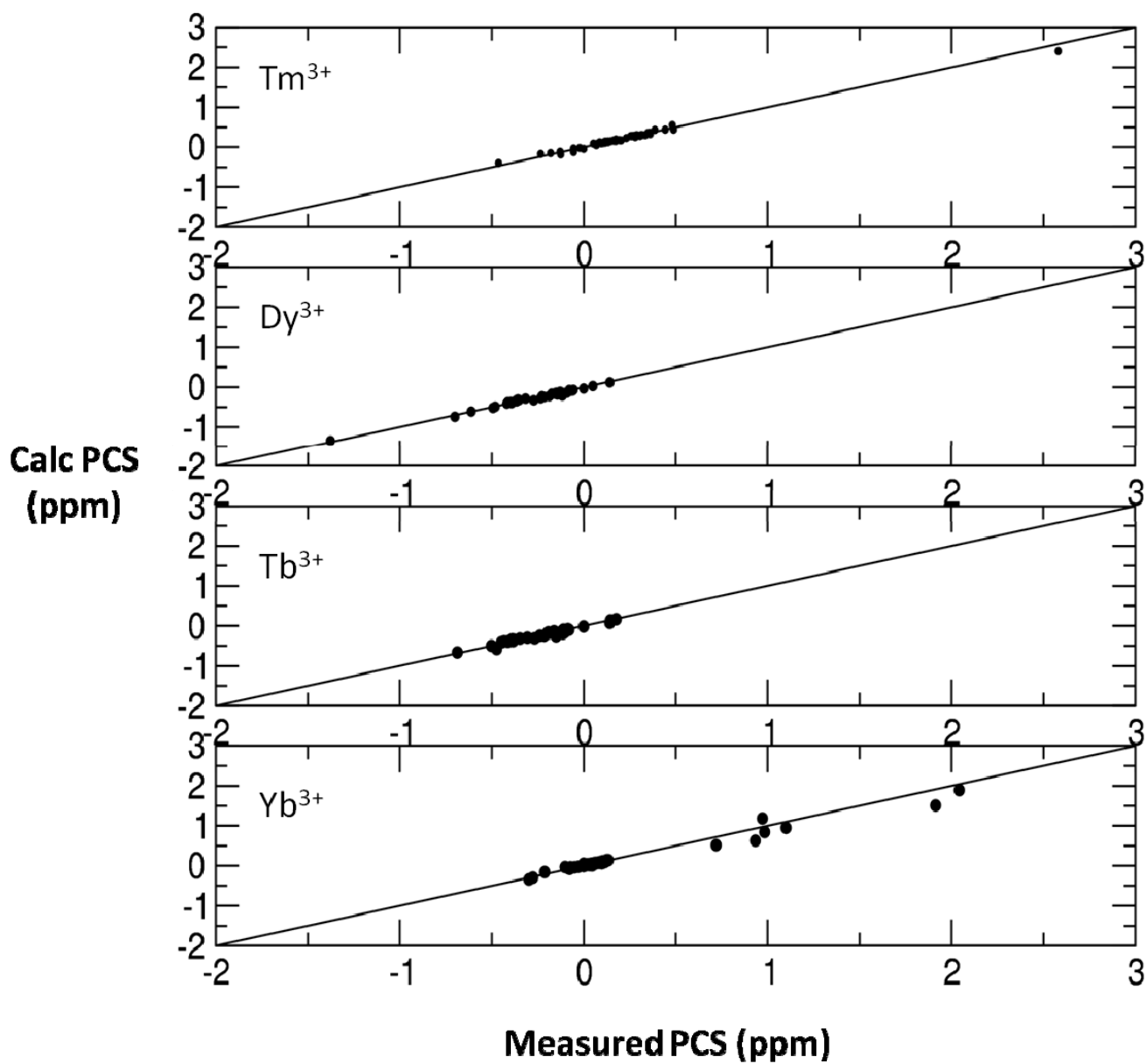


Figure S9. Correlation between measured and back-calculated PCSs for the UbiqE24C/A28C-NTA₂-

Ln³⁺ complexes

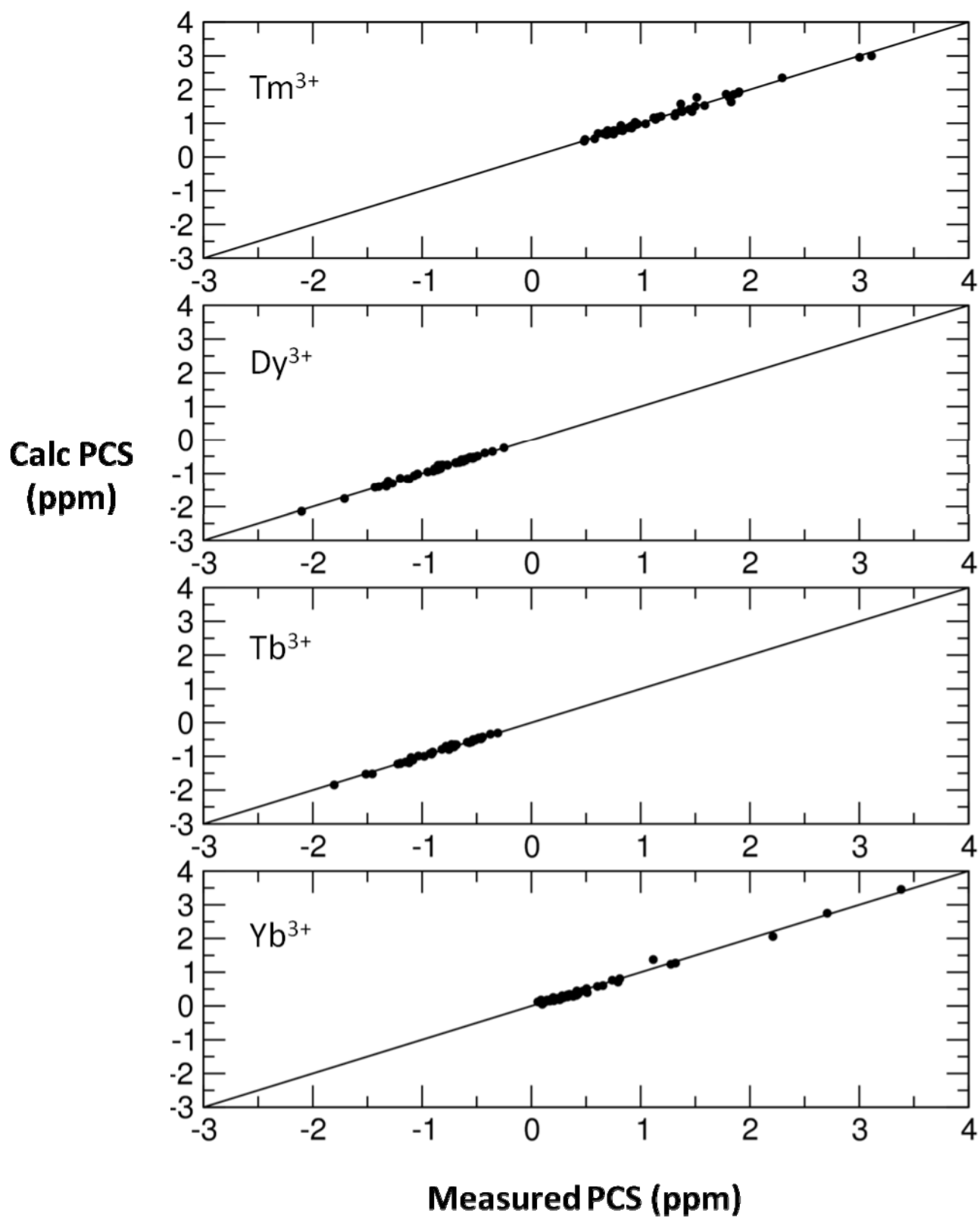
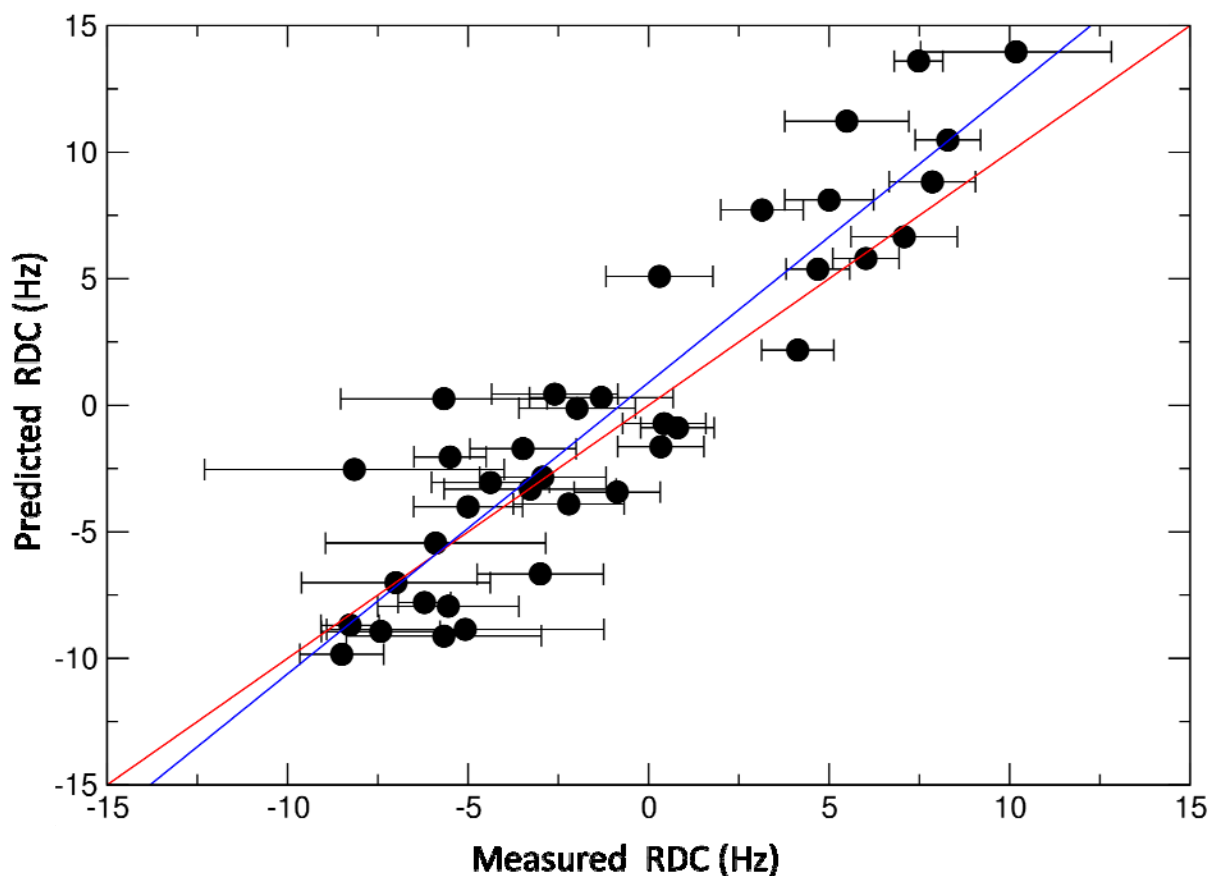


Figure S10. Comparison of measured $^1D_{\text{HN}}$ RDCs and those calculated from the $\Delta\chi$ tensor for the UbiquE24C/A28C-NTA₂-Tm³⁺ complex

The sample was UbiquA28C-NTA loaded with La³⁺/Tm³⁺ recorded at 600 MHz. The blue line shows a linear regression of the data with slope = 1.15.



RDCs were predicted from the $\Delta\chi$ tensor using equation (4) with the order parameter set to 0.9:¹⁴

$$RDC_{AB}^{calc} = - \frac{B_0^2 \gamma_B \gamma_A \hbar S}{120 k T \pi^2 r_{AB}^3} \left[\Delta\chi_{ax} \frac{2z_{AB}^2 - x_{AB}^2 - y_{AB}^2}{r_{AB}^2} + \frac{3}{2} \Delta\chi_{rh} \frac{x_{AB}^2 - y_{AB}^2}{r_{AB}^2} \right]$$

where γ_A and γ_B are the gyromagnetic ratios for spin A and B, \hbar is the Planck constant divided by 2π , S is the order parameter, r_{AB} is the internuclear distance, and x_{AB} , y_{AB} and z_{AB} are the coordinates of the vector **AB** expressed in the $\Delta\chi$ tensor frame of reference.

Figure S11. Comparison of measured $^1D_{\text{HN}}$ RDCs and those calculated for the UbiqE24C/A28C-NTA₂-Tm³⁺ complex recorded at a field strength of 14.1 Tesla

37 RDCs were fitted to the first conformer of the RDC-refined structure of ubiquitin (pdb 1D3Z) using PALES single-value decomposition (SVD) as implemented in the '*bestFit*' module.¹⁸

The following parameters and statistics were obtained:

$D_a = 2.627555 \times 10^{-4}$, $D_r = 7.755643 \times 10^{-5}$. The following two sets of Euler angles were obtained for rotation about x, y, z:

-8.24° , 18.87° , 75.01° and 171.67° , 161.13° , 255.01° .

The uncertainties of measurement (displayed as error bars in the plot) were calculated from SN/LW as reported,¹⁹ and RDCs were measured in the ^{15}N dimension of a ^{15}N fast HSQC⁶ without ^1H decoupling during t_1 .

The goodness-of-fit is reflected in the Q value (19.7%) and the Pearson (R_p) linear correlation coefficient (0.964), as well as the overall r.m.s.d. between measured and calculated RDCs (1.46 Hz).

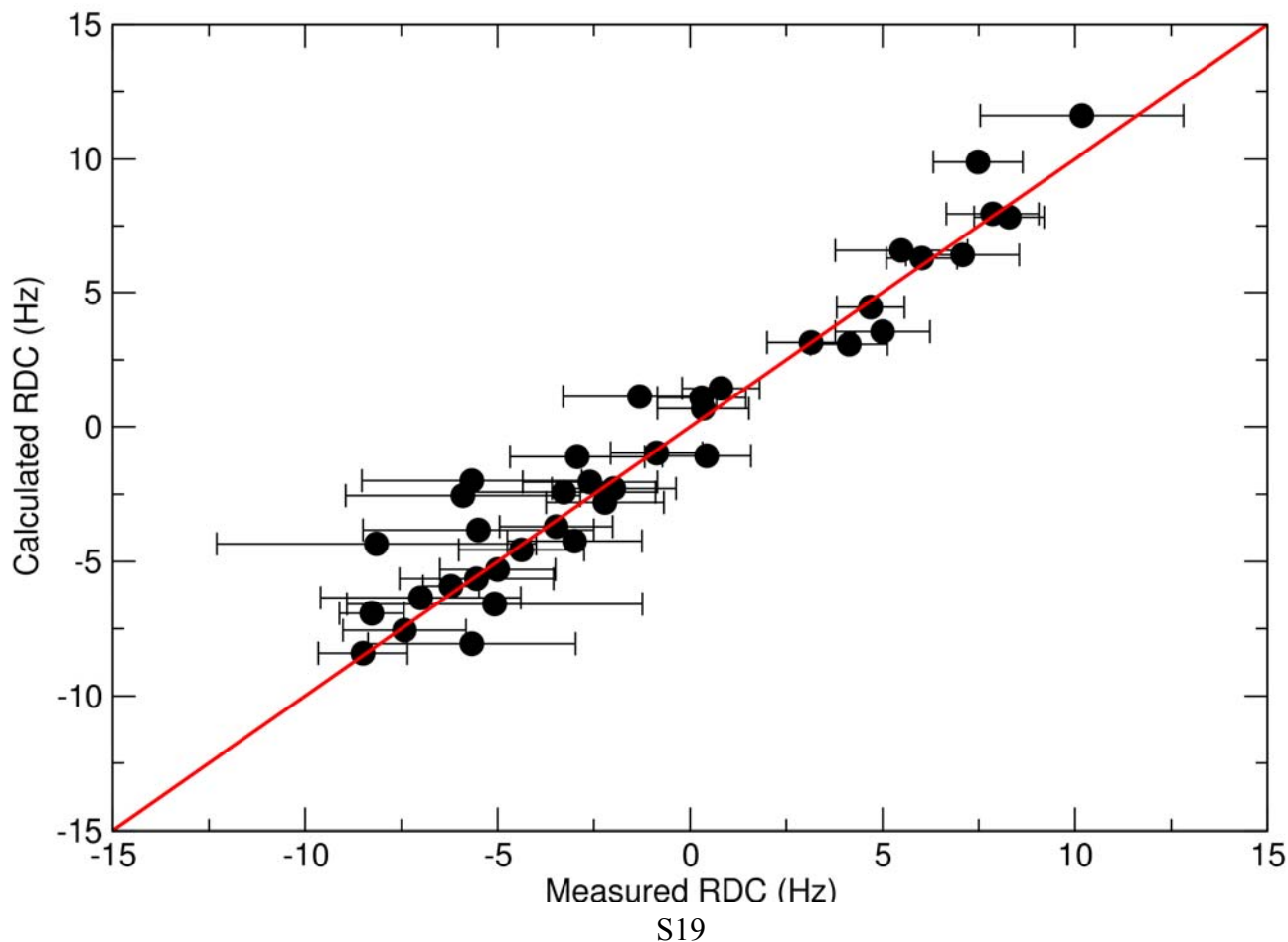
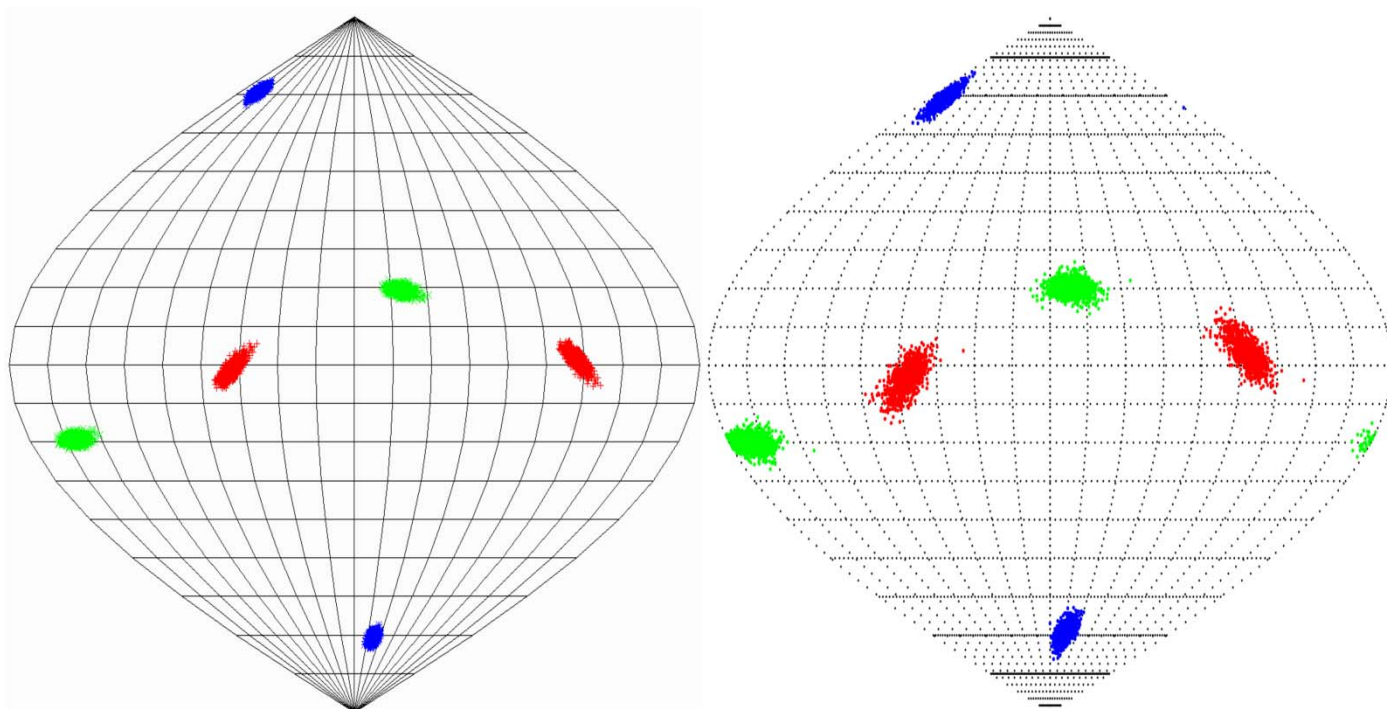


Figure S12. Comparison of the principal axes of the $\Delta\chi$ tensor with those of the RDC-derived alignment tensor for the UbiqE24C/A28C-NTA₂-Tm³⁺ complex, and calculation of the axial component of the RDC-derived $\Delta\chi$ tensor



Orientations of the principal axes of the $\Delta\chi$ (left) and alignment tensor (right), as represented by Sanson-Flamsteed world maps. The points show where the principal axes of the tensors penetrate the sphere with the axes coloured as follows: z (blue), y (red), x (green). For the alignment tensor, 1,000 replicates of SVD calculation using the structural noise Monte-Carlo method ('*mcStruc*' module) within PALES are shown. Similarly, 1,000 Monte-Carlo replicates are shown for the $\Delta\chi$ tensor with 10% structural noise added. The convention $|z| > |y| > |x|$ is used to name the axes. As expected for a rigid metal complex, the orientations of the principal axes of the alignment tensor (right) are very similar to the orientations of the principal axes of the $\Delta\chi$ tensor (left).

The value of the axial ($\Delta\chi_{ax}$) component of the $\Delta\chi$ tensor was calculated from the axial component of the alignment tensor (A_a) obtained by PALES¹⁸ using the following equation:¹³

$$\Delta\chi_{ax} = A_a \frac{15\mu_0 kT}{B_0^2}$$

where B_0 is the field strength (18.8 T), μ_0 is the magnetic permeability of vacuum ($12.566 \times 10^{-7} \text{ T}^2 \text{ m}^3 \text{ J}^{-1}$), k is the Boltzmann constant ($1.38 \times 10^{-23} \text{ J K}^{-1}$), T is temperature (in Kelvin) and $\Delta\chi_{ax}$ is the axial component of the magnetic susceptibility anisotropy tensor (in m^3). The value of A_a (5.3×10^{-4}) was determined by PALES from the best fit of the RDCs, corresponding to a $\Delta\chi_{ax} = 20.5 \times 10^{-32} \text{ m}^3$.

Table S4. Experimentally measured ^1H N PCSs (in ppm) for ArgN-NTA- Ln^{3+} complexes

		Co^{3+}	Dy^{3+}	Tb^{3+}	Tm^{3+}	Yb^{3+}
LEU	10	-0.043	-0.165	-0.160	0.052	
VAL	11	-0.043	-0.292	-0.298	0.035	0.032
LYS	12	-0.043	-0.239			
ALA	13	-0.049	-0.168	-0.144		
PHE	14	-0.121	-0.396	-0.348	0.221	0.081
LYS	15	-0.137	-0.733	-0.662	0.247	0.099
ALA	16	-0.066	-0.322	-0.210		0.050
LEU	17	-0.175			0.393	0.150
LEU	18					0.270
LYS	19					0.430
SER	24					0.124
SER	25					0.208
GLY	27	-0.268	-0.248	-0.230	0.584	0.148
GLU	28	-0.295	-0.047	-0.090	0.533	0.133
ILE	29	-0.328	-0.208	-0.200	0.696	0.179
VAL	30	-0.242	-0.217	-0.200	0.520	0.137
ALA	31	-0.230	-0.011		0.309	0.053
ALA	32	-0.185	0.140	0.070	0.260	0.064
LEU	33	-0.158		-0.020	0.273	0.080
GLN	34	-0.124			0.182	0.050
GLU	35	-0.098	0.140	0.120	0.084	0.040
GLN	36	-0.079	0.140	0.133	0.050	
GLY	37	-0.056	0.079	0.062	0.047	
PHE	38	-0.067	-0.010	-0.020	0.084	0.000
ASP	39	-0.056	-0.047	-0.046	0.085	0.028
ASN	40	-0.062	-0.089	-0.078	0.114	0.031
ILE	41	-0.083	-0.124	-0.112	0.177	0.049
ASN	42	-0.118	-0.267	-0.254	0.294	0.086
SER	44	-0.126	-0.316	-0.303	0.342	0.100
LYS	45	-0.127	-0.371	-0.360	0.348	0.106
VAL	46	-0.181	-0.484	-0.465	0.484	0.144
SER	47	-0.215	-0.643	-0.626	0.613	0.182
ARG	48	-0.137	-0.688	-0.680	0.554	0.167
MET	49	-0.216	-0.828	-0.760	0.600	0.190
LEU	50	-0.328	-1.242	-1.230	0.977	0.300
THR	51	-0.261	-1.309	-1.320	0.938	0.285
LYS	52	-0.254			0.697	0.190
PHE	53	-0.248	-1.533	-1.570	0.815	0.249

The uncertainty for each PCS value was $\pm 0.03\text{ppm}$.

Table S5. Experimentally measured H^N PCSs (in ppm) for UbiquitinA28C/NTA-Ln³⁺ complexes

	Dy ³⁺	Tb ³⁺	Tm ³⁺	Yb ³⁺	
MET 1	-0.116	-0.113	0.086		
GLN 2	-0.143	-0.153	0.131	0.035	
ILE 3	-0.366	-0.389	0.311	0.094	
PHE 4	-0.316	-0.347	0.261	0.065	
VAL 5	-0.365	-0.408	0.361	0.115	
LYS 6	-0.352	-0.379	0.306	0.086	
THR 7	-0.227	-0.238	0.194	0.052	
LEU 8	-0.215	-0.215	0.174	0.054	
GLY 10	-0.126	-0.127	0.106	0.021	
LYS 11	-0.106	-0.108	0.116	0.036	
THR 12	-0.092	-0.104	0.129	0.040	
ILE 13	-0.234	-0.267	0.280	0.097	
THR 14	-0.187	-0.150	0.232	0.082	
LEU 15	-0.413	-0.448	0.359	0.105	
GLU 16	-0.481		0.387	0.134	
VAL 17	-0.392	-0.384	0.272	0.085	
GLU 18	-0.418		0.203	0.063	
SER 20			-0.234	-0.101	
ASP 21			-0.125	-0.072	
THR 22				-0.298	
VAL 26				0.720 ^a	1.100 ^c
LYS 27				0.972 ^a	
LYS 29				2.040 ^a	1.913 ^{b,c}
ILE 30			2.580	0.984 ^a	
GLN 31				0.933 ^b	
GLN 40			0.053		
GLN 41	-1.377		0.489	0.125	
ARG 42	-0.700	-0.687	0.443	0.100	
LEU 43	-0.611	-0.473	0.482	0.102	
ILE 44	-0.397	-0.433	0.360	0.098	
PHE 45	-0.149	-0.192	0.175	0.036	
ALA 46	-0.128	-0.161	0.117	0.024	
GLY 47	-0.079	-0.100	0.131	0.035	
LYS 48	-0.056	-0.086	0.110	0.000	
GLN 49	0.000		0.106	0.000	
LEU 50	-0.126	-0.191	0.256	0.046	
ASP 52			0.000		

	Dy ³⁺	Tb ³⁺	Tm ³⁺	Yb ³⁺
ARG 54				-0.276
THR 55			-0.463	-0.212
LEU 56			-0.055	-0.076
SER 57		0.177	-0.128	-0.075
ASP 58			-0.180	-0.082
TYR 59		0.145	-0.055	-0.050
ASN 60	0.142	0.142	-0.022	-0.030
ILE 61	0.050	0.000	0.069	0.000
GLN 62	-0.078	-0.110	0.095	0.007
LYS 63	-0.061	-0.080	0.070	0.009
GLU 64	-0.163	-0.179	0.145	0.037
SER 65	-0.173	-0.194	0.162	0.031
THR 66	-0.173	-0.199	0.168	0.042
LEU 67	-0.358	-0.394	0.316	0.087
HIS 68	-0.356	-0.387	0.288	0.064
LEU 69	-0.393	-0.416	0.335	0.100
VAL 70	-0.493	-0.502	0.349	0.098
LEU 71	-0.272	-0.306	0.163	0.049

The uncertainty for each PCS value was ± 0.03 ppm. To account for the flexibility of the tag the following tolerances were used for close range PCSs with Yb³⁺: ^a error set to ± 0.2 ppm, ^b error set to ± 0.4 ppm. ^c Measured in the ¹⁵N dimension.

Table S6. Experimentally measured H^N PCSs (in ppm) for Ubiquitin E24C/A28C-NTA₂-Ln³⁺ complexes

		Dy ³⁺	Tb ³⁺	Tm ³⁺	Yb ³⁺
MET 1		-0.248			
GLN 2		-0.353	-0.307	0.579	
ILE 3		-0.766	-0.686	1.136	0.281
PHE 4		-0.860	-0.756	1.187	0.296
VAL 5		-1.040	-0.902	1.373	0.281
LYS 6		-1.042	-0.903	1.379	0.329
THR 7		-0.813	-0.701	1.045	0.259
LEU 8		-0.828	-0.700	0.958	0.209
GLY 10		-0.559	-0.481	0.688	0.162
LYS 11		-0.576	-0.494	0.704	0.152
THR 12		-0.527	-0.457	0.718	0.154
ILE 13		-0.887	-0.768	1.157	
THR 14		-0.625	-0.550	0.971	
LEU 15		-0.830	-0.770	1.320	0.331
GLU 16		-0.535	-0.520	1.120	0.257
VAL 17		-0.525	-0.462	0.915	0.261
GLU 18		-0.691	-0.568	0.819	0.235
SER 20					0.100
ASP 21				0.610	
THR 22					0.906
ILE 23					1.276
VAL 26					2.707
LYS 27					3.383
LYS 29					2.210
ILE 30					1.115
GLN 31					1.319
ASP 32					0.505
LYS 33		-1.340	-1.150		0.330
GLU 34		-1.431	-1.222	1.810	0.345
GLY 35		-1.271	-1.084	1.470	0.294
ILE 36				1.514	0.404
GLN 40				1.900	0.655
GLN 41				3.112	0.809
ARG 42		-1.710	-1.514	2.295	0.604
LEU 43		-2.103	-1.804	3.003	0.793
ILE 44		-1.393	-1.197	1.851	
PHE 45		-0.897	-0.754	1.313	0.383

		Dy³⁺	Tb³⁺	Tm³⁺	Yb³⁺
ALA	46	-0.656	-0.546	0.918	0.263
GLY	47	-0.587	-0.503	0.716	0.144
LYS	48	-0.599	-0.514	0.801	
GLN	49	-0.530	-0.454	0.756	0.174
LEU	50	-1.326	-1.119	1.894	0.474
GLU	51	-1.311	-1.101	1.367	
THR	55	-1.119	-0.913		
LEU	56		-1.455	1.828	0.511
SER	57	-0.949	-0.819	0.661	0.088
ASP	58	-0.830	-0.730		
TYR	59	-0.843	-0.708	0.835	0.194
ASN	60	-0.637	-0.533	0.491	0.059
ILE	61	-0.851	-0.730	0.697	
GLN	62	-0.604	-0.522	0.752	0.206
LYS	63	-0.423	-0.375	0.483	
GLU	64	-0.490	-0.446	0.687	0.171
SER	65	-0.617		0.800	0.186
THR	66	-0.664	-0.587	0.890	0.220
LEU	67	-1.071	-0.927	1.445	0.413
HIS	68	-1.134	-0.980	1.585	0.427
LEU	69	-1.200	-1.034	1.500	0.348
VAL	70	-1.397	-1.198	1.782	0.416
LEU	71	-0.860	-0.781	0.949	
ARG	72				0.284
LEU	73			0.273	0.111
GLY	75			-0.140	

The uncertainty for each PCS value was ± 0.03 ppm.

Table S7. Experimentally measured $^1D_{\text{HN}}$ RDCs (in Hz) for Ubiquitin E24C/A28C-NTA₂-Tm³⁺ complex

		RDC	RDC error
GLN	2	4.13	1.00
ILE	3	0.80	1.01
PHE	4	-5.55	2.00
VAL	5	-7.42	1.60
LYS	6	-7.00	2.60
THR	7	-2.60	1.75
LEU	8	10.18	2.64
GLY	10	0.30	1.15
LYS	11	0.43	1.15
ILE	13	-5.67	2.70
THR	14	-6.21	0.73
LEU	15	0.34	1.19
VAL	17	7.86	1.20
GLU	18	-1.31	1.99
GLU	34	-1.98	1.61
GLY	35	-3.28	2.38
ILE	36	-2.93	1.75
ARG	42	5.00	1.23
ILE	44	-3.48	1.47
PHE	45	-4.38	1.63
ALA	46	-8.15	4.15
LYS	48	-8.27	0.84
GLN	49	-8.50	1.16
LEU	50	-5.67	2.86
GLU	51	-5.90	3.05
SER	57	7.08	1.47
TYR	59	-3.00	1.75
GLN	62	4.69	0.88
LYS	63	-2.21	1.53
GLU	64	6.02	0.92
SER	65	8.29	0.91
THR	66	-0.87	1.19
LEU	67	-5.08	3.84
HIS	68	-5.50	3.00
LEU	69	3.14	1.14
VAL	70	5.49	1.72
LEU	71	7.48	1.16

References

1. E. Masiukiewicz and B. Rzeszutarska, *Org. Prep. Proc. Int.*, 1999, **31**, 571.
2. M. Sunnerhagen, M. Nilges, G. Otting and J. Carey, *Nat. Struct. Biol.*, 1997, **4**, 819.
3. X. C. Su, T. Huber, N. E. Dixon and G. Otting, *ChemBioChem*, 2006, **7**, 1599.
4. J. Cavanagh, W. J. Fairbrother, A. G. Palmer III, M. Rance and N. J. Skelton, *Protein NMR Spectroscopy (Second Edition) Principles and Practice 2007*, Elsevier.
5. C. Brutscher, *J. Am. Chem. Soc.*, 2005, **127**, 8014.
6. S. Mori, C. Abeygunawardana, M. O. Johnson and P. C. van Zijl, *J. Magn. Reson. B.*, 1995, **108**, 94.
7. M. John, M. Headlam, N. E. Dixon and G. Otting, *J. Biomol. NMR*, 2007, **37**, 43.
8. M. Ottiger, F. Delaglio and A. Bax, *J. Mag. Res.*, 1998, **131**, 373.
9. F. Delaglio, S. Grzesiek, G. W. Vuister, G. Zhu, J. Pfeifer and A. Bax, *J. Biomol. NMR*, 1995, **6**, 277.
10. C. Bartels, T.-H. Xia, M. Billeter, P. Güntert and K. Wüthrich, *J. Biomol. NMR*, 1995, **5**, 1.
11. T. D. Goddard and D. G. Kneller, SPARKY 3, University of California, San Francisco.
<http://www.cgl.ucsf.edu/home/sparky/>
12. A. Bax and N. Tjandra, *J. Biomol. NMR*, 1997, **10**, 289.
13. I. Bertini, C. Luchinat and G. Parigi, *Prog. NMR. Spectrosc.*, 2002, **40**, 249.
14. C. Schmitz, M. Stanton-Cook, X.-C. Su, G. Otting and T. Huber, *J. Biomol. NMR*, 2008, **41**, 179.
15. M. Stanton-Cook, X.-C. Su, G. Otting and T. Huber, <http://comp-bio.anu.edu.au/mscook/PPT/>
16. J. Wang, Z. R. Liu, X. D. Zhang and W. G. Jia, *Chem. J. Chin. Univ.*, 2002, **23**, 2052.
17. T. H. D. Nguyen, K. Ozawa, M. Stanton-Cook, R. Barrow, T. Huber and G. Otting, *Angew. Chemie Int. Ed.*, 2011, **50**, 692.
18. M. Zweckstetter, A. Bax. *J. Am. Chem. Soc.*, 2000, **122**, 3791.
19. G. Kontaxis, G. M. Clore, and A. Bax, *J. Magn. Reson.*, 2000, **143**, 184.